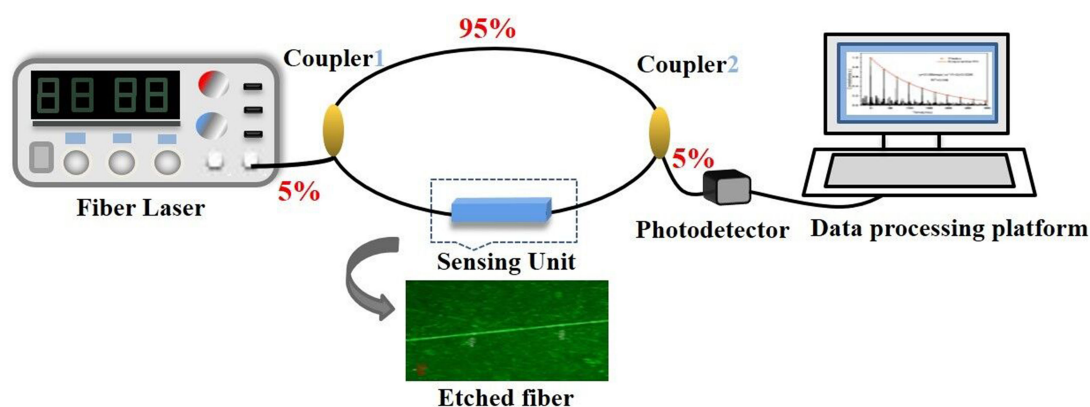


# Formation of Fiber Tapers by Chemical Etching for Application in Chaotic Correlation Fiber Loop Ring Down Sensing

Volume 13, Number 2, April 2021

Tianlong Wu  
Lingzhen Yang  
Jun Tian  
Jie Chen  
Zhuang Liu  
Linlin Fan  
Weijie Ding  
Juanfen Wang  
Pingping Xue



DOI: 10.1109/JPHOT.2021.3065414

# Formation of Fiber Tapers by Chemical Etching for Application in Chaotic Correlation Fiber Loop Ring Down Sensing

Tianlong Wu,<sup>1</sup> Lingzhen Yang ,<sup>1,2</sup> Jun Tian,<sup>1</sup> Jie Chen,<sup>1</sup>  
Zhuang Liu,<sup>1</sup> Linlin Fan,<sup>1</sup> Weijie Ding,<sup>1,3</sup> Juanfen Wang,<sup>1</sup>  
and Pingping Xue<sup>1</sup>

<sup>1</sup>College of Physics and Optoelectronics, Taiyuan University of Technology, Taiyuan 030024, China

<sup>2</sup>Lab of Advanced Transducers and Intelligent Control System, Ministry of Education, Taiyuan University of Technology, Taiyuan 030024, China

<sup>3</sup>Department of Physics, Xinzhou Teachers University, Xinzhou 034000, China

DOI:10.1109/JPHOT.2021.3065414

This work is licensed under a Creative Commons Attribution-NonCommercial-NoDerivatives 4.0 License. For more information, see <https://creativecommons.org/licenses/by-nc-nd/4.0/>

Manuscript received October 13, 2020; revised February 22, 2021; accepted March 7, 2021. Date of publication March 11, 2021; date of current version March 26, 2021. This work was supported in part by the National Natural Science Foundation of China under Grants 61975141, 61575137, and 61675144, and in part by the Shanxi 1331 Project Key Innovative Research Team. Corresponding author: Lingzhen Yang (e-mail: office-science@tyut.edu.cn).

**Abstract:** Fiber loop ring down spectroscopy has been developed into a high-sensitivity technique for sensing many important characteristics of samples, such as refractive index. In contrast to the previous demonstrations by using mode-locked fiber laser, this work is demonstrated to use chaotic laser combined with fiber loop ring down sensor. The formation and performance of fiber tapers was monitored by combining chaotic fiber ring down technology on line and in real time. Two sets of refractive index sensing experiments are performed and further analyzed by using the proposed setup. The results are shown that the detection limit of the chaotic correlation fiber loop ring down system is  $3.45 \times 10^{-4}$  RIU and the sensitivity is  $0.0682 \text{ ns}^{-1} \text{ RIU}^{-1}$  in 6.7 m, respectively. The performance of our system can be drastically improved by increasing the length of the etched fiber tapers to be tens of centimeters using the chaotic correlation fiber loop ring down system with the smaller fiber ring lengths.

**Index Terms:** Chaotic laser, fiber loop ring down, etched fiber tapers, refractive index.

## 1. Introduction

Refractive index (RI) sensor plays an important role in the field of water quality monitoring. Many RI sensors using optical tapers have been studied in the last years such as Fiber-Taper Seeded Long-Period Grating Pair with a sensitivity of the 35.9 nm/RIU sensitivity [1], Bent Optical Fiber Taper with a sensitivity of 1506 nm/RIU [2]. These sensors are based on the measurement of spectrum and intensity.

Fiber loop ring down spectroscopy (FLRDs) was proposed by Stewart et al. in 2001 [3]. It's a variant of cavity ring down spectroscopy (CRDs) [4] and has the advantages of fast response, high sensitivity and insensitivity to the fluctuations of laser source. The components of the sensor

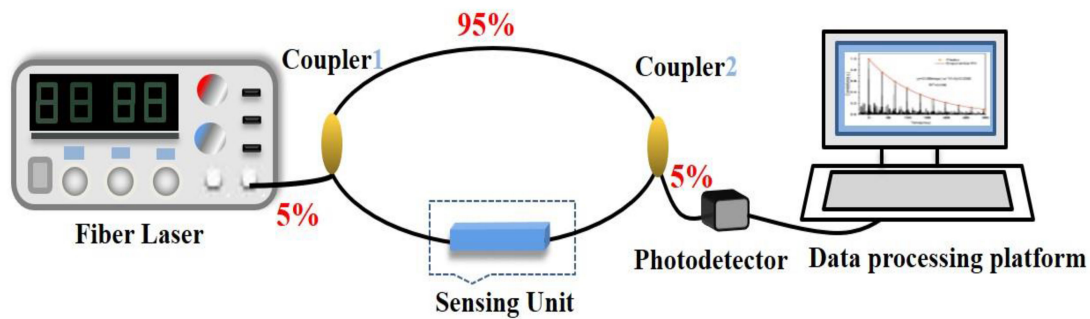


Fig. 1. Schematic diagram of the etched fiber tapers-FLRD sensing system.

such as optical microfiber coupler or long period fiber grating can be welded in FLRD system for sensing such as the gases sensor [5], biosensors [6], temperature sensor [7], strain sensor [8] and refractive index (RI) sensor [9]. Recent years, the application of evanescent field (EF) structure to reduce the complexity of sensor head in sensing fields has attracted more researchers.

In the EF structure sensing fields, the methods for removing the cladding of the fiber, such as side polishing [10], thermal tapering [11] and chemical etching [12] are well-known to improve the sensitivity by inducing the evanescent field. The side polishing method can provide high-precision quantitative fiber size while the process is really costly; The thermal tapering head is easy to use, but is limited in the manufacture of long tapered fibers. The etching method allows the production of uniform fiber surfaces with very long length. Under a certain concentration of chemical solution, the etching process can be controlled by virtue of the contact time of the fiber surface.

Recently, the etched fiber tapers as sensor in FLRD setup have been reported. The ring down time of light intensity was measured in FLRDs with the two couplers so that it can effectively reduce the influence of the intensity fluctuation of the injected pulse [13]. Wang, et al. proposed high-sensitivity refractive index sensor by FLRD technique [14]. Jiang, et al. proposed precise measurement of liquid level by FLRD technique [15]. For the pulsed FLRDs, the pulse is generally composed of the intensity modulator, the laser source and the signal generator [16], [17]. The frequency of the intensity modulator must ensure that there is only one set of pulses in the fiber loop. Due to the trade-off problem between the frequency and width of the pulse, the length of fiber loop needs to be considered [18] and the ring down time is also greatly influenced by the narrower pulse width [19], [20].

With the advantages of high frequency, broad bandwidth and intrinsic randomness, chaotic laser has the potential applications for sensing. The chaotic correlation FLRDs have been reported in our group [7], [21]. By measuring the e-exponential decay of the peak value of correlation of the chaotic laser, high-sensitivity sensing could be achieved. In this paper, we report on the formation and sensing of the fiber tapers with the chemical etching method based on chaotic correlation FLRDs. The etching process can be controlled in real time by combining the FLRD technique and scanning electron microscopy (SEM). Meanwhile, the effect of different length and diameter for fiber tapers on sensor performance are investigated. Finally, the more sensitive fiber tapers is used for refractive index sensing and compared with the pulsed FLRDs under different fiber ring lengths.

## 2. Experimental Setup and Principle

As shown in Fig. 1, the FLRDs sensing setup is seeded by a chaotic fiber laser [21]. The sensing part consists of two 95:5 couplers, the etched sensor and the single mode fiber (SMF). The chaotic fiber laser is injected into the fiber loop cavity through coupler 1 and circulates cyclically inside the fiber loop cavity. The attenuated laser is exported out of the loop through coupler 2 and is detected by the detector and collected by data processing platform. The experiment results are processed the data acquisition system in real time.

When the physical quantity changes, such as RI around the etched sensor, it cause the change in the ring down time [22], [23]. The principle can be modeled by:

$$B = \frac{n_c L}{c} \left( \frac{1}{\tau_R} - \frac{1}{\tau_{R0}} \right) = t_r \left( \frac{1}{\tau_R} - \frac{1}{\tau_{R0}} \right) \quad (1)$$

where  $\tau_{R0}$  is the autocorrelation coefficient ring down and  $\tau_R$  is the ring down time with the additional loss  $B$ ;  $t_r$  is defined as the travel time of the light in the loop. When the light pass through the etched sensor, it is assumed that the  $B$  is caused exclusively by EF attenuation. By analyzing the EF scattering  $\gamma_\beta$ , absorption  $\gamma_\alpha$ , or both of them [24], the (1) can be further expressed as:

$$B_{EF} = t_r \left( \frac{1}{\tau_R} - \frac{1}{\tau_{R0}} \right) = L_e (\gamma_\alpha + \gamma_\beta) \quad (2)$$

where  $L_e$  is the etched fiber length of the sensor, the change of the EF loss could be caused by some parameters, such as the diameter of the fiber tapers and EF penetration depth. The diameter and length of the etched fiber tapers will be the parameters we want to control in our work.

To test the performance of the etched sensor, sodium chloride solutions were prepared for RI sensing. The relationship between  $B$  and refractive index  $n$  and detailed theory have been described in our previous work [25]. Chaotic signals only have correlation peaks and it means the correlation between the sequences of chaotic signals at other moments is almost equal to 0. So, the ring down time is measured by detecting the peak of correlation function in the chaotic FLRDs, which is different from detecting the pulse peak in the pulsed FLRDs.

The chaotic fiber laser is used to carry out the experiment. The output power is 35 mW in the experiment. The central wavelength is 1550 nm which is presented in Fig. 2(a). The noise-like time series can be obtained in Fig. 2(b). The autocorrelation curve with the properties of delta-like-function is obtained in Fig. 2(c). Fig. 2(d) demonstrates a fitted exponential decay curve of chaotic autocorrelation coefficient and the ring down time is 114 ns. The loop ring length of the experiment is 6.7m by observing the round trip time of 33 ns between adjacent peaks of the autocorrelation curve.

### 3. Results and Discussion

The etched fiber is fabricated as follows. The plastic jacket of the certain fiber in the fiber loop was removed and putted into a 40% hydrofluoric acid (HF) solution. Fig. 3 demonstrates the real time monitoring process. The relationship between ring down time and etching time was fitted. The cladding of the fiber was gradually etched and thinned. With the EF interaction between the surface of fiber and the HF solution, the ring down time began to change. The etching time lasted about 53 min from points A-C in Fig. 3. When the etching effect reaches our expectations, the etched fiber should be cleaned immediately to dilute the HF solution and reduce the etching rate. Then the fiber was put into the ultrasonic bath to remove the remaining HF solution on the end surface to prevent the further corrosion. The etched fiber is encapsulated in a U-shape glass tube with glass epoxy to facilitate subsequent measurements. The experimental solution tank is made by a 3D printer and the laboratory temperature is controlled at 23°C. It should be noted that it is necessary to pay attention to the corrosive time and the etched fiber should be cleaned with deionized (DI) water and dried for a while if not the residual HF can further corrode the fiber and even the fibers are all corroded.

The etching process can be controlled by observing the ring down time. For quantitative measurement, the SEM was used to measure the size of the etched fiber in different time periods of the etching process. According to the etching process in Fig. 3, SEM imaging of the fiber diameter at different times was conducted. It can be seen from the SEM images in Fig. 4, the diameters of the etched fiber tapers were 91  $\mu\text{m}$ , 72  $\mu\text{m}$  and 45  $\mu\text{m}$  corresponding to the B, D and E respectively in the process as shown in Fig. 3. The observed ring down times of these three points were 461 ns, 338 ns and 240 ns. Meanwhile, we can use (2) to calculate the EF losses at points B, D and E are

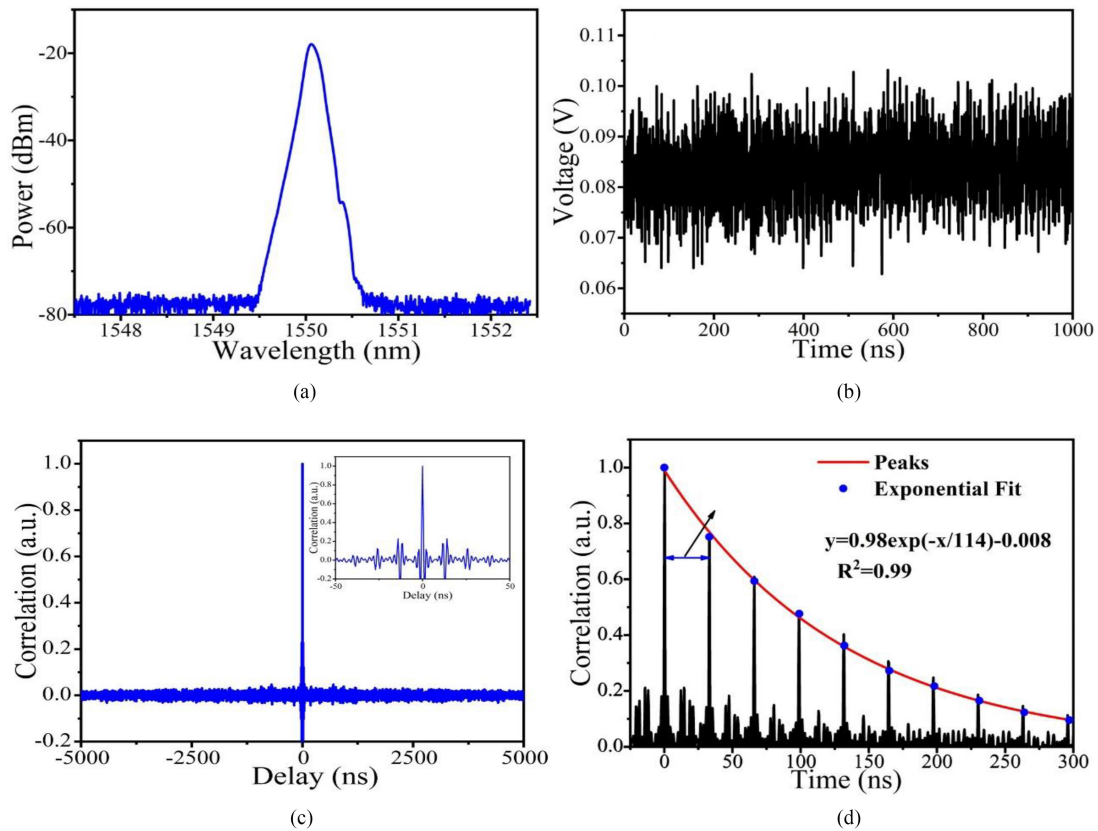


Fig. 2. (a) Chaotic laser spectrum. (b) time series of chaotic fiber laser. (c) autocorrelation curve. (d) autocorrelation curve of the decayed chaotic laser.

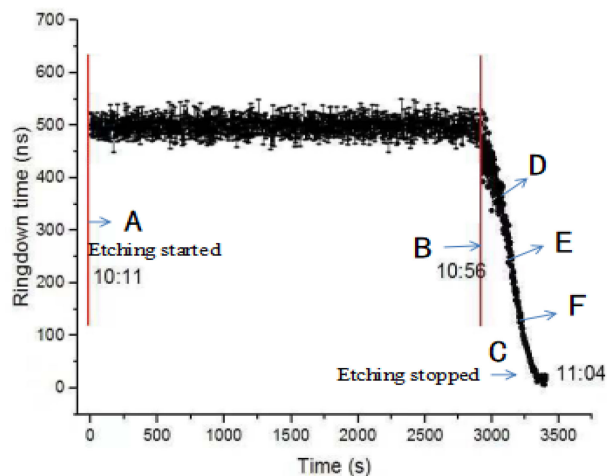


Fig. 3. On line and real-time monitoring of the etching process.

0.56% (0.024 dB), 3.12% (0.133 dB) and 7.15% (0.322 dB), respectively. The results demonstrate that the losses caused by EF interaction are inversely proportional to the etched fiber diameter.

The relationship between etched fiber diameter and ring down time are fitted to a curve as shown in Fig. 5. The fitting curve shows that a longer ring down time corresponding to a larger etched fiber diameter, a lower EF loss. When the corrosion time reaches a certain point, it is equivalent to B

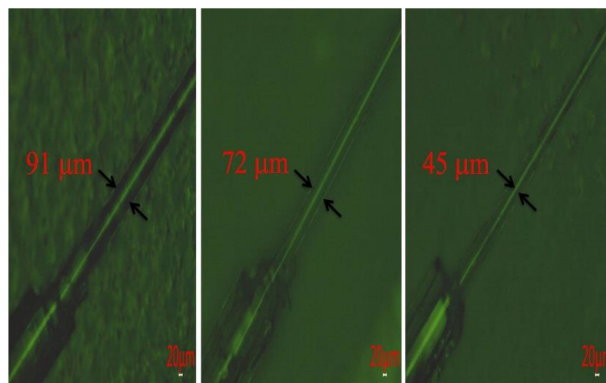


Fig. 4. Scanning electron microscopy imaging of B, D, E three-point fiber diameter.

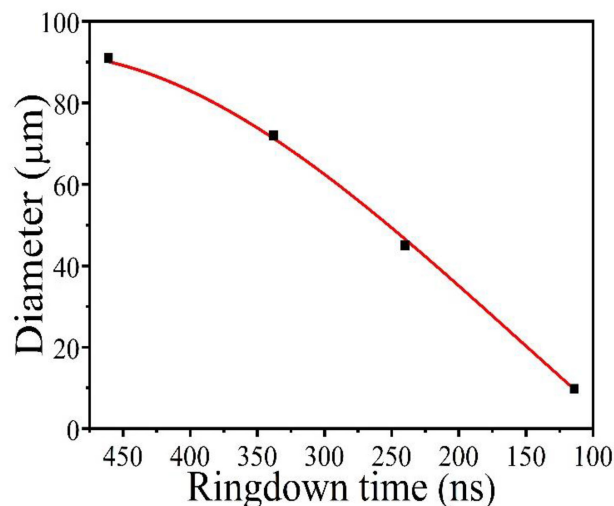


Fig. 5. The ring down time varies with the diameter of the etched fiber.

in Fig. 3. The thinner the fiber diameter with the longer the etching time causes the fiber loss to increase and the smaller the ring down time. The results show that SEM imaging combined with FLRD technology can be used to observe the ring down time to estimate the diameter of the etched fiber tapers. It's meaningful that FLRDs can be a powerful tool to control the fabrication of the sensor heads with different diameters in real time to achieve sensing.

The different lengths of the etched fiber tapers to achieve the desired sensitivity was further fabricated when the diameter is determined. The fiber length segments 3 cm and 5 cm with diameter of  $9.2 \mu\text{m}$ , were etched separately and labeled. The different concentrations of the sodium chloride solution was prepared in the laboratory. The experiment refractive index (RI) are 1.335, 1.340, 1.345, 1.350, 1.356, 1.361, 1.366, 1.372 [26]. For each measurement, an appropriate amount of the solution is poured into the experimental solution tank until the sensor element is completely immersed.

Fig. 6 shows the linear relationships between the  $(1/\tau_R - 1/\tau_{R0})$  and RI tested by two sensor heads with different length. The sensitivities of the two sensor heads are  $0.0682 \text{ ns}^{-1}\text{RIU}^{-1}$  and  $0.0529 \text{ ns}^{-1}\text{RIU}^{-1}$ , respectively. It can be seen from that  $(1/\tau_R - 1/\tau_{R0})$  linearly increases with the increase of the RI, and the etched fiber tapers with longer length has better sensitivity. The results show that the sensor head's sensitivity is proportional to the length of the etched fiber tapers and the fabrication of the fiber tapers with different length can be controlled to achieve different sensitivities. The etched fiber tapers with 5 cm length was selected for further analysis.



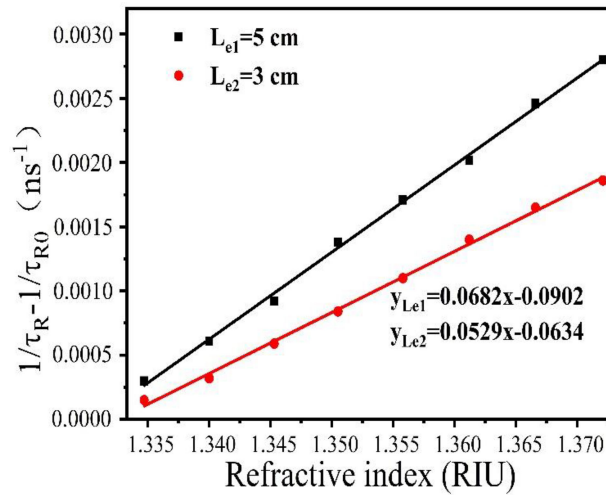


Fig. 6. The relationships between the  $(1/\tau_R - 1/\tau_{R0})$  and RI tested by two etched fiber tapers with different length.

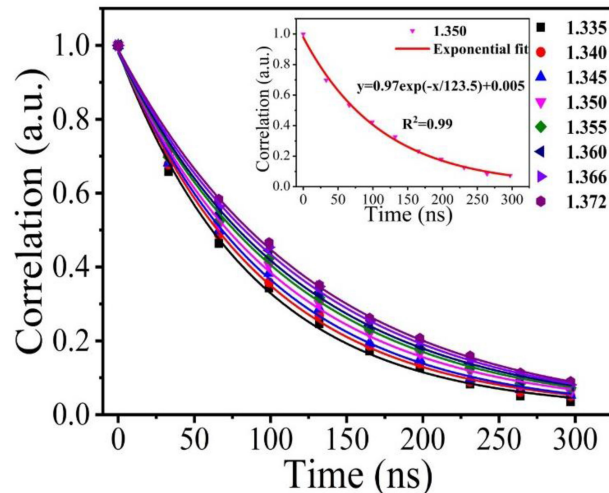


Fig. 7. Autocorrelation coefficient evolution under different RI with the 5 cm length etched fiber.

The peaks of the attenuation curve were extracted and fitted into an exponential curve in chaotic signal processing as shown in Fig. 7. The evolution curve of the autocorrelation coefficient under different RI with the 5 cm length etched fiber explains the fast measurement method of the chaotic correlation FRLDs.

The performance and detection limit (DL) of the pulsed FLRDs and the chaotic correlation FLRDs have been compared experimentally using 5 cm length etched fiber tapers with diameter of  $9.2 \mu\text{m}$ . The fiber ring to chaotic and pulsed light source are connected respectively. The experimental setup based on chaotic laser has been introduced above. The experimental device based on pulsed laser as shown in Ref [27] and the pulses generated by the mode-locked fiber laser are coupled into fiber loop. Experimental data of chaotic light with a ring length of 6.7 meters were collected in Table 1, but no signal was found when the same ring was connected to the pulse source. This is because the output light pulse will overlap making it impossible to sense when the round trip time ( $t_r$ ) in the fiber loop is smaller than pulse light width. The pulsed light requires a larger fiber ring length. Then we changed the length of the fiber ring. And the display of the pulse signal can be seen when the fiber ring is increased to 20 m. We know the fiber loop length usually needs

TABLE 1.  
Performance Comparison of the Chaotic Correlation FLRDs and the Pulsed FLRDs

Parameter	Chaotic correlation FLRDs		Pulsed FLRDs
Length of the cavity (L) (m)	6.7	20	20
Ring down time (tr(ns))	33	97.3	97.1
Standard error in ring down time ( $\Delta \tau$ ) (ns)	$1.38 \times 10^{-5}$	$1.82 \times 10^{-5}$	$4.51 \times 10^{-5}$
Slope	0.0682	0.0363	0.0482
Detection limit (RIU)	$3.45 \times 10^{-4}$	$5.01 \times 10^{-4}$	$9.36 \times 10^{-4}$

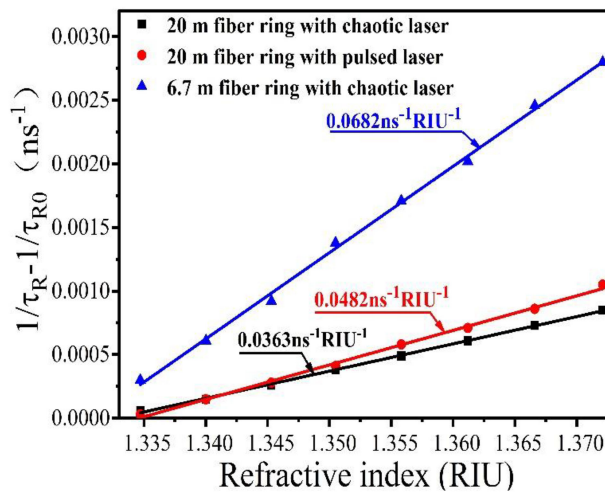


Fig. 8. Comparison of sensitivity of chaotic laser and pulsed laser under different fiber ring lengths.

to be hundred to thousand meters in the pulsed FLRDs [9], [14]. The changes of pulsed signal by data acquisition system in real time was observed and the results confirm that the chaotic correlation FLRDs supports shorter fiber loop to a few meters. We also connect the fiber ring cavity to pulsed light source under the length of 20 m. The results are shown in Fig. 8 and Table 1. Fig. 8 shows the relationships between the  $(1/\tau_R - 1/\tau_{R0})$  and RI tested within the RI range of 1.335-1.375. It is found that  $(1/\tau_R - 1/\tau_{R0})$  has an excellent linear relationship with the RI, and  $(1/\tau_R - 1/\tau_{R0})$  increases significantly with the increase of RI. The standard deviation, sensitivity and detection limit (DI) were calculated in Table 1. When we connect the fiber ring to pulsed light source, the sensitivity is  $0.0482 \text{ ns}^{-1} \text{ RIU}^{-1}$ . The standard error is  $4.51 \times 10^{-5}$  and the DI is  $9.36 \times 10^{-4}$  RIU.

The same fiber ring to chaotic laser was demonstrated, the sensitivity is  $0.0363 \text{ ns}^{-1} \text{ RIU}^{-1}$  lower than the sensitivity of the pulsed FLRDs, but the standard error is  $1.82 \times 10^{-5}$  which is about one third comparing to the pulsed FLRDs. And the DI is  $5.01 \times 10^{-4}$  RIU lower than the pulsed FLRDs. This means the DI has been increased roughly doubled comparing to the pulsed FLRDs. These data are also recorded in Table 1. We compare the data under three different experimental conditions in Table 1. It is found that the standard error in chaotic correlation FLRDs in 6.7 m is  $1.38 \times 10^{-5}$  and DI is  $3.45 \times 10^{-4}$  RIU. The sensitivity in chaotic correlation FLRDs in 6.7 m is  $0.0682 \text{ ns}^{-1} \text{ RIU}^{-1}$ . Compared with measuring spectrum and intensity, RI sensing is achieved by measuring more sensitive ring down time variations and low cost in our experiment. The sensitivity



can be further improved by shortening the length of the loop. On the other hand, the sensitivity is improved gradually as the decrease of the fiber loop length. Compared with the pulsed FLRDs, the chaotic light has strong anti-interference ability and very broad bandwidth which contribute to its lower noise of the basement and lower DI. The sensitivity and DI of the sensor can be further improved by increasing the coupling ratio of the coupler or adding amplification compensation in the fiber loop cavity.

#### 4. Conclusion

In conclusion, a fiber detecting system using etched structure combined with FLRDs based on chaotic laser is proposed. This real time monitoring method for etching fiber has shown great prospects in many practical applications that require on line and lower cost. Moreover, the pulsed and chaotic FLRDs refractive index sensing was carried out using a more sensitive sensor element under different fiber ring lengths. The results show the standard error in chaotic correlation FLRDs in 6.7 m is the lowest and the sensitivity is the highest. Comparing to the mature pulsed FLRD technique, the chaotic correlation FLRDs supports shorter fiber loop length due to the extremely narrow bandwidth characteristic of the chaotic autocorrelation and the method of measuring the autocorrelation correlation. The results further elucidate the potential in monitoring the concentration of toxic liquids, especially for liquids with higher RI than the fiber cladding, such as gasoline, methanal and chemical solutions.

---

#### References

- [1] J. F. Ding, A. P. Zhang, and L. Y. Shao, "Fiber-taper seeded long-period grating pair as a highly sensitive refractive-index sensor," *IEEE Photon. Technol. Lett.*, vol. 17, no. 6, pp. 1247–1249, Jun. 2005.
- [2] C. R. D. Silveira, "Bent optical fiber taper for refractive index measurements with tunable sensitivity," *Microw. Opt. Technol. Lett.*, vol. 57, no. 4, 2015.
- [3] G. Whitenett, G. Stewart, K. Atherton, P. Shields, and B. Culshaw, "An investigation of an optical fiber amplifier loop for intra-cavity and ring-down cavity loss measurements," *Meas. Sci. Technol.*, vol. 12, no. 7, pp. 843, 2001.
- [4] L. van der Sneppen, F. Ariese, C. Gooijer, and W. Ubachs, "Liquid-phase and evanescent-wave cavity ring-down spectroscopy in analytical chemistry," *Annu. Rev. Anal. Chem.*, vol. 2, no. 1, pp. 13–35, 2009.
- [5] Y. Zhao *et al.*, "Novel gas sensor combined active fiber loop ring-down and dual wavelengths differential absorption method," *Opt. Exp.*, vol. 22, no. 9, pp. 11244–11253, 2014.
- [6] K. Zhou, D. Webb, and M. Farries, "Biochemical sensor based on a novel all-fiber cavity ring down spectroscopy technique incorporating a tilted fiber Bragg grating," *Opt. Laser. Eng.*, vol. 47, no. 10, pp. 1032–1027, 2009.
- [7] C. Qin, L. Yang, and J. Yang, "Temperature sensing based on chaotic correlation fiber loop ring down system," *Opt. Fiber Technol.*, vol. 47, pp. 141–146, 2019.
- [8] Z. Wang, M. Jiang, and H. Xu, "New optical fiber micro-bend pressure sensors based on fiber-loop ringdown," *Procedia Eng.*, vol. 29, pp. 4234–4238, 2012.
- [9] D. Wu, Y. Zhao, and Q. Wang "SMF taper evanescent field-based RI sensor combined with fiber loop ring down technology," *IEEE Photon. Technol. Lett.*, vol. 27, no. 17, pp. 1–1, Sep. 2015.
- [10] D.-R. Lee, K.-M. Cho, S.-W. Jang, and D.-H. Kwon, "Side-polished fiber optic temperature sensor using a prism and fiber-to-planar waveguide coupler," *Microw. Opt. Technol. Lett.*, vol. 46, no. 6, pp. 523–525, 2005.
- [11] T. K. Yadav, R. Narayanaswamy, and Bakar, and M. H. A., "Single mode tapered fiber-optic interferometer based refractive index sensor and its application to protein sensing," *Opt. Exp.*, vol. 22, no. 19, pp. 22802–22807, 2014.
- [12] T. K. Gangopadhyay, A. Halder, and S. Das, "Fabrication of tapered single mode fiber by chemical etching and used as a chemical sensor based on evanescent field absorption," *Int. Soc. Opt. Eng.*, vol. 8173, no. 1, pp. 817321–817310, 2010.
- [13] T. V. Lerber and M. W. Sigrist, "Cavity-ring-down principle for fiber-optic resonators: Experimental realization of bending loss and evanescent-field sensing," *Appl. Opt.*, vol. 41, no. 18, pp. 3567–3575, 2002.
- [14] C. Wang and C. Herath, "High-sensitivity fiber-loop ringdown evanescent-field index sensors using single-mode fiber," *Opt. Lett.*, vol. 35, no. 10, pp. 1629–1631, 2010.
- [15] Y. Jiang, W. Jiang, and B. Jiang, "Precise measurement of liquid-level by fiber loop ring-down technique incorporating an etched fiber," *Opt. Commun.*, vol. 351, pp. 30–34, 2015.
- [16] Q. Wang, X. Liu, J. Xia, and Y. Zhao, "A novel long-tail fiber current sensor based on fiber loop ring-down spectroscopy and Fabry – Perot cavity filled," *IEEE Trans. Instrum. Meas.*, vol. 64, no. 7, pp. 2005–2011, Jul. 2015.
- [17] N. Ni, C. C. Chan, and L. Xia, "Fiber cavity ring-down refractive index sensor," *IEEE Photon. Technol. Lett.*, vol. 20, no. 16, pp. 1351–1353, Aug. 2008.
- [18] D. J. Passos, S. O. Silva, J. R. A. Fernandes, and M. B. Marques, "Fiber cavity ring-down using an optical time-domain reflectometer," *Photonic Sensors*, vol. 4, no. 4, pp. 295–299, 2014.

- [19] X. Li, X. Wang, P. Niu, J. Zhao, C. Zhang, and E. Gu, "Refractive index measurement using OTDR-based ring-down technique with S fiber taper," *Opt. Commun.*, vol. 446, pp. 186–190, 2019.
- [20] W. C. Yan, Q. Han, Y. Chen, H. Song, X. Tang, and T. Liu, "Fiber-loop ring-down interrogated refractive index sensor based on an SNS fiber structure," *Sensors Actuators B Chem.*, vol. 255, pp. 2018–2022, 2018.
- [21] L. Yang *et al.*, "Optical sensors using chaotic correlation fiber loop ring down," *Opt. Exp.*, vol. 25, no. 3, pp. 2031, 2017.
- [22] K. Sharma, M. I. M. Abdul Khudus, S. U. Alam, S. Bhattacharya, D. Venkitesh, and G. Brambilla, "Comparison of detection limit in fiber-based conventional, amplified, and gain-clamped cavity ring-down techniques," *Opt. Commun.*, vol. 407, pp. 186–192, 2018.
- [23] K. Sharma, D. Venkitesh, S. Bhattacharya, B. Srinivasan, and G. Brambilla, "Non-linear behavior of ring-down time in cavity ring-down spectroscopy with tapered fibers," in *Proc. Conf. Lasers Electro-Opt., OSA Tech. Dig.*, 2016, Paper JW2A.12.
- [24] A. W. Synder and J. D. Love, *Optical Waveguide Theory*. Norwell, MA, USA: Kluwer Academic, 2000.
- [25] J. Tian, L. Yang, C. Qin, and T. Wu, "Refractive index sensing based on chaotic correlation fiber loop ring down system using tapered fiber," *IEEE Sensors J.*, vol. 20, no. 8, pp. 4215–4220, Apr. 2020.
- [26] W. M. Haynes *et al.*, "Thermochemistry, electrochemistry, and solution chemistry," *CRC Handbook of Chemistry and Physics*, 2012, pp. 5–129.
- [27] Y. Yang, L. Yang, and Z. Zhang, "Fiber loop ring down for static ice pressure detection," *Opt. Fiber Technol.*, vol. 36, pp. 312–316, 2017.